

1 **Seasonal evolution of natural radionuclides in two rivers affected by acid mine drainage and phosphogypsum**

2 **pollution**

3 José Luis Guerrero ^{a,*}, Isidoro Gutiérrez-Álvarez ^a, Almudena Hierro ^a, Silvia M. Pérez-Moreno ^a, Manuel Olías ^b, Juan
4 Pedro Bolívar ^a

5 ^a Department of Integrated Sciences, Center for Natural Resources, Health and Environment (RENSMA), University of
6 Huelva, 21071, Huelva, Spain. E-mail addresses: joseluis.guerrero@dfa.uhu.es (J.L. Guerrero)
7 isidoro.gutierrez@dfa.uhu.es (I. Gutiérrez), almudena.hierro@gmail.com (A. Hierro), bolivar@uhu.es (J.P. Bolívar).

8 ^b Department of Geodynamics and Palaeontology, Center for Natural Resources, Health and Environment (RENSMA),
9 University of Huelva, 21071, Huelva, Spain. E-mail address: manuel.olias@dgyp.uhu.es (M. Olías)

10 *Corresponding author. E-mail address: joseluis.guerrero@dfa.uhu.es. Phone number: +34 959 21 9798. Postal address:
11 Department of Integrated Sciences, Center for Natural Resources, Health and Environment (RENSMA), University of
12 Huelva, 21071, Huelva, Spain.

13 **Abstract**

14 The Odiel and Tinto rivers show singular characteristics due to the significant acid mine drainage (AMD) generated in
15 the first section of their basins and the phosphogypsum (PG) stacks located on their common estuary. AMD leads to
16 low pH and high redox potential, which keep high amounts of toxic elements and radionuclides in dissolution. The
17 objective of this work was to analyse the seasonal evolution of U-Th isotopes and ²¹⁰Po in these rivers and the estuarine
18 mixing zone. Four sampling points were selected (a fluvial point and an estuarine one for each river) and water samples
19 were collected monthly throughout a year. The concentrations of natural radionuclides in the dissolved and particulate
20 phases were determined by alpha spectrometry. The Odiel and Tinto rivers show concentrations of U-Th isotopes and
21 ²¹⁰Po from one to three orders of magnitude higher than background continental waters due to the strong effect of AMD,
22 and ²³⁴U/²³⁸U activity ratios up to 2.

23 The studied radionuclides show a clear seasonal behaviour in these rivers, with three different stages during the year: 1)
24 concentration peaks observed during November and December due to the "washing effect" produced by the first rainfalls
25 of the hydrological year, 2) a "dilution effect" by runoff in the rainy winter, and 3) a progressive "concentration effect"
26 during the spring and summer. A non-conservative behaviour of the analysed radionuclides in the estuaries was
27 demonstrated due to precipitation processes produced by the increase of pH. The polluted outflows from the PG stacks
28 located in the Tinto estuary produce a significant radioactive impact, mainly during the rainiest months, increasing the
29 concentration of U-isotopes and ²¹⁰Po in the particulate phase.

30 **Keywords**

31 Natural radionuclides, acid mine drainage, phosphogypsum, non-conservative, water mixing

32 **1. Introduction**

33 The Tinto and Odiel rivers are located in southwest Spain in the province of Huelva. They present marine influence in
34 their final reach, converging in the common Huelva estuary (Fig. 1). The Tinto River is 101 km long while the Odiel
35 River is 140 km long, and their catchments cover 1600 and 2300 km², respectively. These rivers and their estuary have
36 a great hydrochemical and environmental interest due to two factors. The first is the extensive acid mine drainage (AMD)
37 affecting both rivers because of the existence of several old abandoned sulfide mines in their basins and second is the
38 large chemical industrial complex and phosphogypsum (PG) stacks located by the Huelva estuary.

39 Regarding the AMD, these rivers drain one of the biggest metallogenic regions of massive sulfides in the world: the
40 Iberian Pyritic Belt (IPB). Mining works date from the year 2500 B.C. in this region, although the large-scale
41 exploitation of these deposits took place during the nineteenth and twentieth centuries (Leblanc et al., 2000). The sulfide
42 deposits are predominately composed of pyrite (FeS₂, > 90% of volume), with variable amounts of sphalerite (ZnS),
43 chalcopyrite (CuFeS₂) and galena (PbS) (Sáez et al., 1999; Venkateswarlu et al., 2016). The exposure of these sulfides
44 to oxygen and water liberates sulfate ions and metals and leads to acidity (pH = 2.5-3.0), polluting the waters (Cánovas
45 et al., 2007). There are few works worldwide about concentrations and behaviour of natural radionuclides in locations
46 affected by AMD, but high activity concentrations in these polluted environments have been found mainly for U-
47 isotopes (Fernandes et al., 1998; Yamamoto et al., 2010; Durand, 2012; Madzivire, et al., 2014). In the study area some
48 previous works also shown large concentrations of natural radionuclides with enhanced contents of U-Th isotopes and
49 ²¹⁰Po in both waters and sediments (Hierro et al., 2012, Hierro et al., 2013, Blasco et al., 2016, Manjón et al., 2019a).

50 The AMD confers extreme physicochemical conditions on these rivers, which maintain high concentrations of toxic
51 elements in solution (Cánovas et al., 2007; Nieto et al., 2007; Hierro et al., 2014) and radionuclides (Hierro et al., 2013).
52 When these pollutants arrive at the Huelva estuary, they produce a severe environmental impact (Vicente-Martorell et
53 al., 2009; Cánovas et al., 2010; Sánchez-Moyano et al., 2010). The differences between the physicochemical parameters
54 of the marine and fluvial waters produce a strong pH gradient in the estuarine mixing zone due to the neutralization of
55 these acidic waters and the precipitation of heavy metals and other pollutants from the dissolved into the particulate
56 phase (Achterberg et al., 2003; Braungardt et al., 2003; Hierro et al., 2013, 2014). It is important to take into account
57 that this mixing process does not occur at a steady point. A spatial displacement has been demonstrated, and while

58 during the dry seasons the mixing takes place in the most internal zones of the estuary, during the wet seasons this
59 process takes place in sectors closer to the coast (Carro et al., 2011).

60 The five phosphoric acid plants included in the chemical industrial complex located on the Huelva estuary generated
61 around 100 Mt of a waste called phosphogypsum (PG) between 1968 and 2010, which is stored in large piles on the
62 salt-marshes of the Tinto River covering an area about 1000 ha (Fig. 1). PG is generated during the production of
63 phosphoric acid, and is essentially composed of gypsum ($\text{CaSO}_4 \cdot 2\text{H}_2\text{O}$) but contains high concentrations of ^{238}U series
64 natural radionuclides and other impurities such as P_2O_5 ($\text{pH} \approx 1.5$), F, and toxic metals (Pérez-López et al., 2007; Bolívar
65 et al., 2009). The high concentration of natural radionuclides of PG comes from the raw material used in the industrial
66 process, which in the case of Huelva was sedimentary phosphate rock from Morocco (Bolívar et al., 1996). This
67 phosphate rock contains U-series radionuclide concentrations of around 1500 Bq kg^{-1} (≈ 50 times higher than
68 unperturbed soils), with ^{238}U in radioactive equilibrium with its daughters. About 20% of the U, more than 70% of the
69 Th, and the majority of the Ra, Pb and Po ($> 95\%$) contained in the phosphate rock remain in the PG after the industrial
70 process (Bolívar et al., 1996; Bolívar et al., 2009). Therefore, PG is currently considered a Naturally Occurring
71 Radioactive Material (NORM) (IAEA, 2003; Directive 2013/59/Euratom). On the other hand, the remaining phosphoric
72 acid trapped between the PG particles explains the high acidity and polluting potential of the aqueous leachates produced
73 by this waste (Pérez-López et al., 2010; Pérez-Moreno et al., 2018).

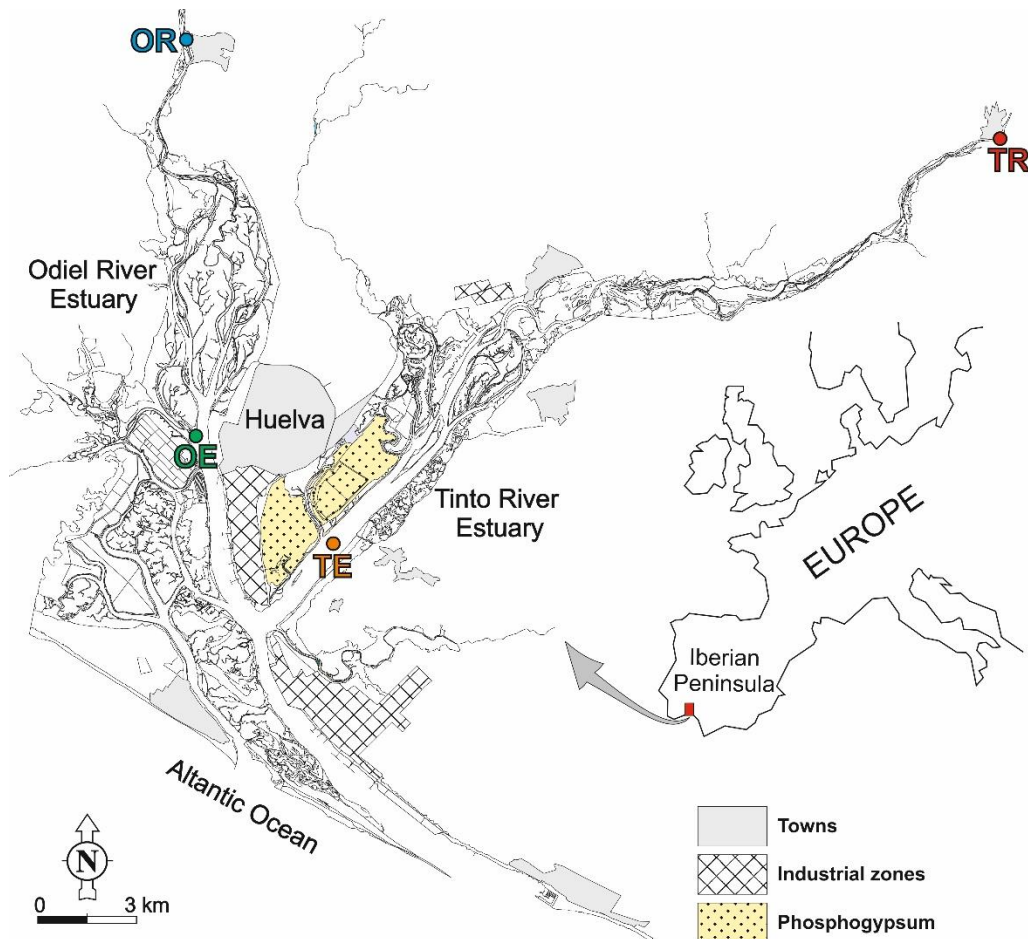


Figure 1. Map of the study area showing the sampling points: Odiel River (OR), Odiel Estuary (OE), Tinto River (TR), and Tinto Estuary (TE).

Until 1998, about 20% of the generated PG was discharged into the Odiel River channel, while the remaining 80% was pumped in suspension with seawater into the stacks, where PG was decanted, and the polluted acidic ($\text{pH} \approx 2$) seawater (around $10^7 \text{ m}^3 \text{ year}^{-1}$) was released into the Tinto River channel without any treatment (Bolívar et al., 2000). From 1998 until the end of the production (31 December 2010), due to a change in the environmental policy according to the OSPAR convention (OSPAR, 2002, 2007), all the PG was pumped with fresh water in a closed circuit and placed into the piles, which reached around 30 m in height in some sectors. The northern and southern areas of the stacks (around 550 ha) have been partially restored (Más et al., 2006). Nevertheless, there are several points where the acidic polluted waters from the PG piles (restored and unrestored) are reaching the waters of the Tinto estuary (Pérez-López et al., 2015, 2016; Papaslioti et al., 2018).

Considering these facts, the aim of this work is to study the concentrations and behaviour of U-Th isotopes and ^{210}Po during a year in the acidic mining waters of these rivers and their polluted estuaries.

2. Material and methods

89 For this study, four sampling points were selected: OR and TR are located in the Odiel and Tinto rivers, while OE and
90 TE are located in the Odiel and Tinto estuaries, respectively. OR and TR represent fluvial composition without any
91 marine influence. At these four points, water samples were collected monthly throughout a year (from October 2009 to
92 September 2010). In total, 48 water samples of 10 L each were collected. Temperature, pH, electrical conductivity (EC)
93 and redox potential (Eh) were measured *in situ* using a Crison MM40+ portable multimeter, with a 5048 (Ag/AgCl)
94 electrode. The instruments were calibrated before sampling, and the redox potential was corrected to obtain the potential
95 relative to the hydrogen electrode (Eh) according to Nordstrom and Wilde (1998).

96 Water samples were filtered in the laboratory by using polycarbonate filters 9.0 cm in diameter with a pore size of 0.45
97 μm . Concentrated HNO_3 was added to achieve $\text{pH} < 2$ in order to prevent the adsorption of radionuclides onto the
98 container walls. The filters were dried and weighed, and the particulate matter (PM) content was calculated by
99 subtracting the filter mass. The filters were cleaned with HNO_3 , and the liberated particulate matter was dissolved by
100 applying atmospheric acid digestion with aqua regia (3 HCl:1 HNO_3). The dry residue was re-dissolved in 8 M HNO_3 .
101 Major and minor elements were determined in the dissolved matter by Inductively Coupled Plasma Optical Emission
102 Spectroscopy (ICP-OES) and Inductively Coupled Plasma Mass Spectroscopy (ICP-MS) at Actlabs (Canada). The
103 quality control (QC) was developed by the measurement of Certified Reference Materials (CRMs) and a duplicate every
104 ten samples.

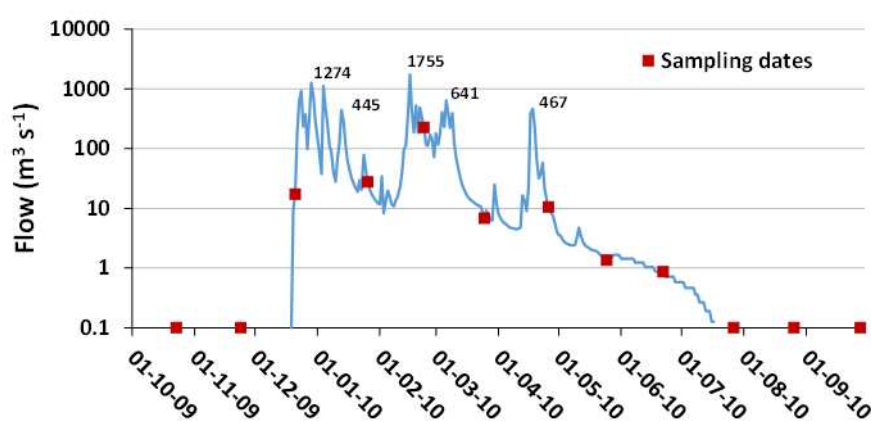
105 Radionuclides in dissolved and particulate matter were determined by a sequential extraction technique based on the
106 use of tributylphosphate (TBP) (Bolívar et al., 2000), subsequent electrodeposition onto a stainless-steel disc (U-Th
107 isotopes) and selfdeposition onto a silver disc (^{210}Po), and measurement of the activities by α -spectrometry using ion-
108 implanted silicon detectors (Bolívar et al., 2000) with 25% absolute efficiency. The QC for alpha-particle measurements
109 was conducted by participating in annual international proficiency tests (International Atomic Energy Agency [IAEA]
110 and the Spanish Nuclear Safety Council [CSN]), and by measuring both a blank and CRMs for every set of six samples
111 (IAEA-443).

112 **3. Results and discussion**

113 **3.1 Fluvial discharges**

114 Rainfall in the province of Huelva is very irregular, with high intra- and interannual variability. This irregularity in the
115 precipitation together with the low permeability of the Tinto and Odiel river basins explains the large variations in the
116 flow of these rivers (Olías et al., 2006). The rainfall is concentrated throughout the wet season, between the months of
117 October and April, preceded by the low flow-season between the months of May and September. The average annual

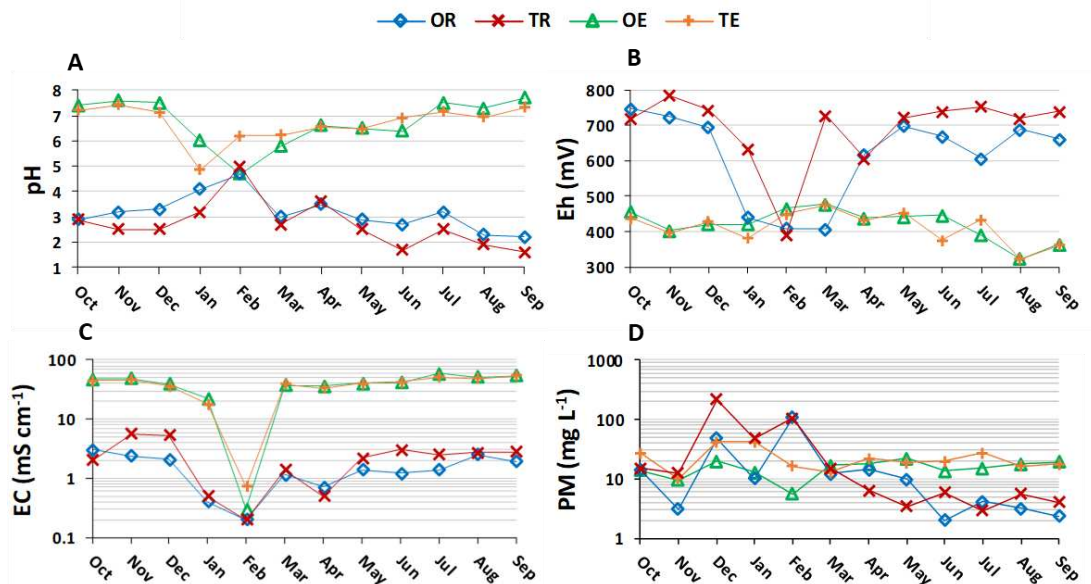
118 flows of the Odiel and Tinto rivers are 29 and 1.6 m³ s⁻¹ respectively (Olías et al., 2006), but the flows can increase by
119 up to two orders of magnitude during floods, mainly in the autumn and winter months.
120 The average rainfall recorded during the study period at meteorological stations located close to the fluvial sampling
121 points (OR and TR) was very high (960 mm) compared to the average rainfall in the area (550 mm). The highest
122 precipitations were registered in the winter months, with occasional rain during the spring and very low rainfall during
123 the summer and autumn months (Fig. S1 of the supplementary material). Figure 2 shows the Odiel River flow data
124 recorded in the stream gauging station close to the OR sampling point (unfortunately, there are no data for the Tinto
125 River flow). It should be noted that during the autumn there was no flow in the Odiel River, which is unusual since
126 November is normally one of the rainiest months. The highest flows, like the precipitations, were recorded during the
127 winter months with a maximum in February (1755 m³ s⁻¹).



128
129 Figure 2. Daily flow of the Odiel River during the study period indicating the sampling dates

130 3.2 Hydrochemistry

131 The measured physicochemical characteristics are in Table S1 of the supplementary material. The pH of the Odiel and
132 Tinto rivers shows the acidity of their waters during the year, with median pH values of 3.2 and 2.7, respectively. The
133 lower pH in the Tinto River is due to the greater impact produced by the AMD on its course (Olías et al., 2004). In both
134 estuaries, the pH values are very similar and notably higher than the fluvial ones, with almost neutral mean values (OE
135 = 7.0, TE = 6.9) due to the influence of the seawater (pH ≈ 8). Regarding the temporal evolution (Fig. 3A), the behaviour
136 of the pH at the estuarine points (OE and TE) is opposite to that in the rivers (OR and TR). This is explained by the fact
137 that the intense rain decreases the acidity of the rivers during the winter and spring months due to the dilution effect by
138 runoff. On the other hand, the large discharge of fluvial water during these months (mainly January and February)
139 displaces the seawater out of the estuaries, making the marine influence less important and increasing the acidity of their
140 waters (Fig. 3A).



141

142

143

144

145

146

147

148

149

150

151

152

153

154

155

156

157

158

159

160

Figure 3. Evolution of pH (A), redox potential (B), electrical conductivity (C) and particulate matter (D) during the year in the riverine and estuarine sampling points.

The Eh showed the same mean value (≈ 420 mV) in both estuaries, similar to the value of seawater (400-435 mV) (Kennish, 2017), while in the rivers it is significantly higher (OR = 613 and TR = 689 mV) (Fig. 3B). Under these oxidising conditions, U is found primarily as U(VI) in the form of the highly soluble uranyl ion UO_2^{2+} , which forms complexes mainly with carbonate and phosphate under neutral conditions or with sulfate and fluorides at acidic pH values (Porcelli and Swarzenski, 2003), while under reducing conditions, uranium is predominantly present as U(IV) and tends to precipitate as insoluble minerals. In the rivers, the Eh decreased significantly during the winter months due to the dilution effect caused by rainfall, while in the estuaries it remained more or less constant during the year.

The mean values of EC in the fluvial waters were 1.5 and 2.4 mS cm^{-1} at the sampling points OE and TE, respectively, showing the large amount of dissolved ions transported by these rivers. The higher EC of the Tinto River is consistent with its higher acidity. In the estuaries the mean EC was around 40 mS cm^{-1} , slightly lower than the typical EC of seawater (50 mS cm^{-1}), as expected due to the mixing. The temporal evolution of the EC (Figure 3C) shows a similar pattern to the pH, with a large decrease during the rainy season (around two orders of magnitude) due to the great intake of fluvial water, mainly in February.

The particulate matter (PM) showed similar concentrations at both estuarine points with a mean of 15 and 23 mg L^{-1} in the Odiel and Tinto estuaries, respectively. At fluvial sampling points the median concentration was around 10 mg L^{-1} , with significant higher values (> 100 mg L^{-1}) during the winter months in relation to flood events, which produce an increase in the water turbidity (Fig. 3D).

161 The concentrations of major and trace elements in the dissolved phase are listed in Tables S2-S5 of the supplementary
 162 material, showing the values at the sampling points. The high concentrations of sulfate and metals in these rivers are
 163 due to the effects of AMD. The mean sulfate concentrations in the Odiel and Tinto rivers were 970 and 1550 mg L⁻¹,
 164 respectively. The metals and metalloids with the highest concentrations at the fluvial sampling points were the following
 165 (mean concentration in brackets): Al (OR = 58 and TR = 86 mg L⁻¹), Zn (OR = 15 and TR = 21 mg L⁻¹), Mn (OR = 11.9
 166 and TR = 8.6 mg L⁻¹), Cu (OR= 5.3 and TR=18.9 mg L⁻¹) and Fe (OR = 7.5 and TR = 144 mg L⁻¹). All these elements
 167 decrease their concentrations in the rivers by around one order of magnitude after flood events (January, February, and
 168 April in this study) due to the dilution effect and increase their concentrations during the dry season (Tables S2 and S3).
 169 At the estuarine points, the compositions of the waters are clearly influenced by seawater and are very similar to one
 170 another. The measured species with higher concentrations and their mean values (in brackets, mg L⁻¹) are as follows:
 171 Na (OE = 7800 and TE = 7400), SO₄²⁻ (OE = 2200 and TE = 2100), Ca (OE = 300 and TE = 330), K (OE and TE =
 172 330), and Sr (OE and TE = 5.4). Several metals (Al, Fe, Cr, Pb, Sn) showed concentrations below the DL during the
 173 year. Almost all metals increase their concentrations in the estuaries by around one order of magnitude during the rainiest
 174 months due to the higher fluvial flow, while the elements with higher concentrations in seawater notably decrease their
 175 concentrations during these periods (Tables S4 and S5). These concentrations and behaviour agree with previous studies
 176 (Olías et al., 2006; Cánovas 2007; Hierro et al., 2014).

177 In order to know the influence of the rivers on their estuaries during the year, the percentages of fluvial water in this
 178 mixing zone were determined based on the conservative behaviour of Na (Loder and Reichard, 1981; Gordeev and
 179 Lisitzin, 2014), according to:

$$180 \quad \% \text{ fluvial water} = \frac{[X_{\text{Na}}(\text{E})] - X_{\text{Na}}(\text{SW})}{[X_{\text{Na}}(\text{R})] - X_{\text{Na}}(\text{SW})} \cdot 100 \quad (1)$$

181 where X_{Na}(E) and X_{Na}(R) are the concentrations of Na at the estuarine and fluvial sampling points, respectively, and
 182 X_{Na}(SW) is the approximate concentration of Na in seawater (10⁴ mg L⁻¹). These percentages are displayed in Figure
 183 4. The high percentage of fluvial water at the estuarine points during the rainy season is noteworthy, mainly after the
 184 flood events of January (49 and 62% in the Odiel and Tinto estuaries, respectively), February (≈ 99% in both estuaries)
 185 and April (37 and 44% in the Odiel and Tinto estuaries, respectively). These values demonstrate the similarity between
 186 these two systems and the fact that the mixing zone is not spatially steady during the year; on the contrary, during the
 187 wet season, the mixing process takes place towards more outward sectors.

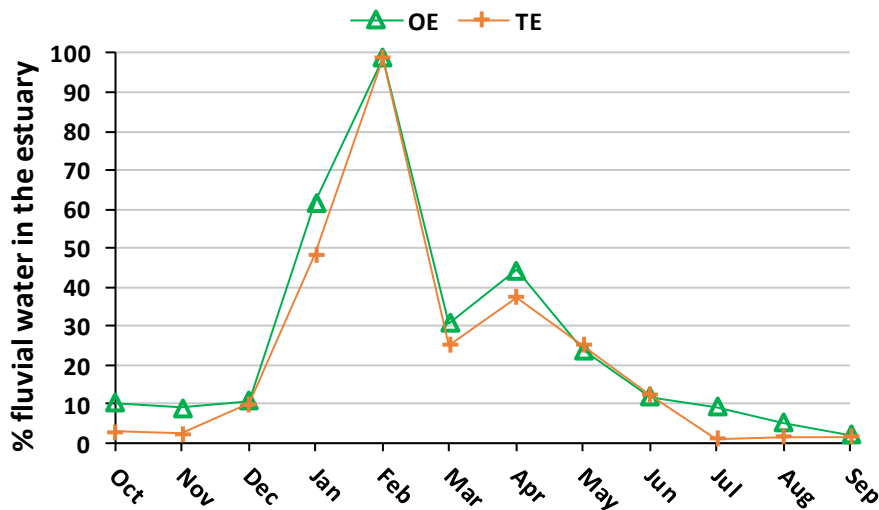
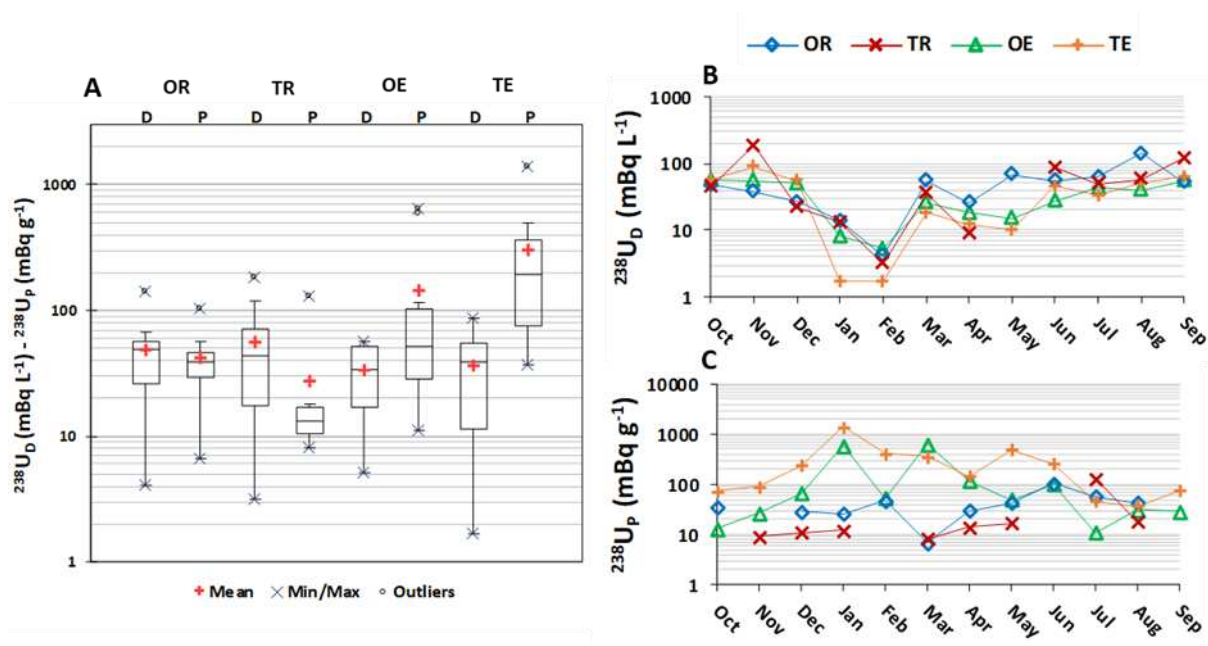


Figure 4. Percentage of river water in the estuarine sampling points.

3.3 Natural radionuclides

3.3.1 U-isotopes

The ^{238}U activity concentrations for the dissolved and particulate matter are displayed as box and whiskers plots in the Figure 5A, and the temporary evolution is shown in Figure 5B and C. Data are shown in Table S6 of the supplementary material. The mean concentrations in the dissolved phase were 49 and 57 mBq L^{-1} in the Odiel and Tinto rivers, respectively, approximately 10 times higher than the background values of continental surface waters in Europe (around 4 mBq L^{-1}) and worldwide (6 mBq L^{-1}) (De Vos and Tarvainen, 2006). In the estuaries, the dissolved ^{238}U activity concentrations are similar, with means of 33 and 36 mBq L^{-1} for the Odiel and Tinto estuaries, respectively (Fig. 5A), slightly lower than the mean for marine water (40 mBq L^{-1} ; Ku et al., 1977). Nevertheless, concentrations higher than 50 mBq L^{-1} were reached, mainly in the Tinto estuary.



201 Figure 5. Box whisker plots of ^{238}U concentration in the dissolved and particulate phases (A), and temporal evolution
202 for the dissolved (B) and particulate phases (C). Central line: median; box limits: first and third quartiles; whiskers:
203 minimum and maximum non-outliers.

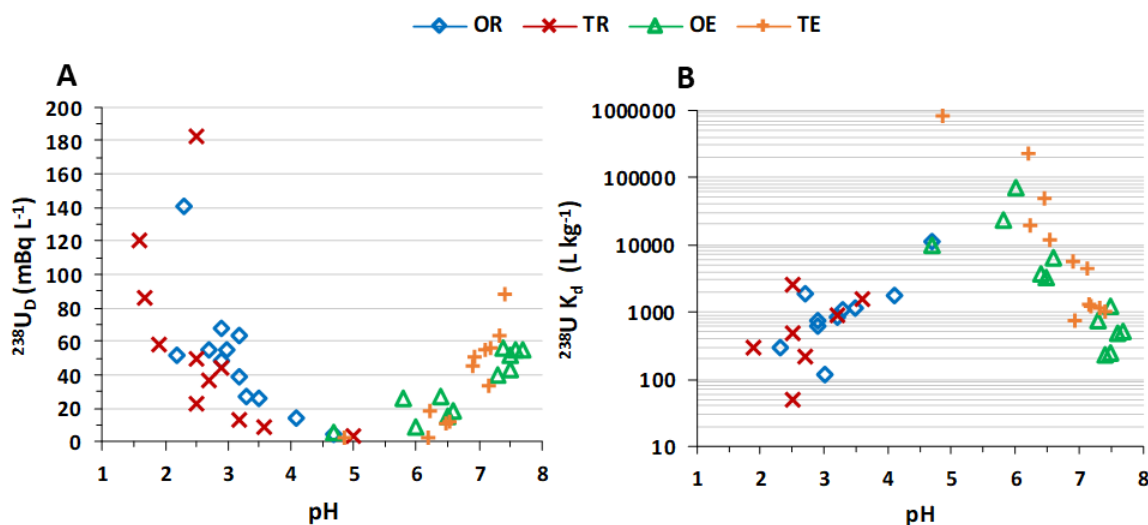
204 According to Figure 5B and taking into account the obtained uncertainties, which were lower than 10% (Table S6 of
205 the supplementary material), the dissolved ^{238}U shows a clear seasonal pattern in both rivers and estuaries with an
206 important decrease during the winter months because of the dilution effect during the rainy season. During the rainiest
207 months, an additional U input in the Tinto estuary should be considered: the lateral polluted outflows from the PG stacks,
208 which show a mean concentration of ^{238}U of $4.5 \cdot 10^4 \text{ mBq L}^{-1}$ (Pérez-Moreno et al., 2018), because of the surface runoff
209 and groundwater. The dissolved activity concentrations increase progressively during the dry season at all the sampling
210 points due to the decrease in the river flows (Figure 2). While the maximum concentration for the Odiel River was
211 measured in the month of August ($140 \pm 4 \text{ mBq L}^{-1}$), the Tinto River reached its maximum in November ($182 \pm 13 \text{ mBq}$
212 L^{-1}). This peak of dissolved ^{238}U in the Tinto River is related to the dissolution of the efflorescences precipitated during
213 the dry season by the first rainfalls of the hydrological year (Cánovas et al., 2007).

214 In the particulate matter, the mean ^{238}U concentrations at the fluvial points were 42 and 27 mBq g^{-1} in the Odiel and
215 Tinto rivers, respectively, while in the estuaries they were significantly higher, at 143 and 300 mBq g^{-1} in the Odiel and
216 Tinto estuaries, respectively (Figure 5C). The ^{238}U concentration in the particulate matter of the estuaries is one order
217 of magnitude higher than the worldwide median concentration in unperturbed sediments, which is 35 mBq g^{-1} with a
218 range from 16 to 110 mBq g^{-1} (UNSCEAR, 2000). The high concentration of this radionuclide in the Tinto estuary is
219 probably related with the releases from the PG stacks. The particulate ^{238}U activity concentration does not show a
220 seasonal pattern as clearly as the dissolved one. The highest activity concentrations in the particulate matter of the
221 estuaries were observed during the rainy season, with $\approx 600 \text{ mBq g}^{-1}$ in January and March in the Odiel estuary and \approx
222 1400 mBq g^{-1} in February in the Tinto estuary, probably due to the decrease of pH in the estuaries and consequent
223 coprecipitation/sorption of dissolved U, as discussed below. This behaviour is not observed at the fluvial points, which
224 show more or less constant concentrations during the year, with the highest values ($> 100 \text{ mBq g}^{-1}$) during the summer
225 months.

226 The percentage of ^{238}U associated with the particulate matter at the sampling points was determined (Table S7 of the
227 supplementary material). In general, the particulate ^{238}U shows low percentages in both rivers, below 2% in most cases,
228 with a median value of around 1%, which indicates that it is mainly transported in the dissolved phase. During the winter
229 months, a notable increase of this percentage is observed, with a maximum of 55% in the Odiel River in February,

230 probably due to the high rainfall in this month, and therefore an increase in pH to around 5 (Fig. 3A), producing the U
 231 precipitation. Unfortunately, the particulate matter in the Tinto River in this month was not determined. In the estuaries,
 232 the percentage of ^{238}U associated with the particulate matter is notably higher than the fluvial one, with means of 9 and
 233 25% in the Odiel and Tinto estuaries, respectively. The maximum values for both estuaries were reached in January,
 234 and were 49% in the Odiel River and up to 97% in the Tinto River.

235 The relationship between the pH and the dissolved ^{238}U activity concentration and the distribution coefficients (K_d) is
 236 shown in Figure 6, where it can be observed that the concentration of ^{238}U decreases as pH increases in the rivers. The
 237 lowest ^{238}U activity concentrations in the dissolved phase ($< 30 \text{ mBq L}^{-1}$) were observed in the pH range from 4 to 6,
 238 which are reached during the rainy season in both rivers and estuaries as previously mentioned. For pH values higher
 239 than 6, which are observed in the estuarine points mainly during the dry season, the dissolved ^{238}U again increases its
 240 concentration, reaching values above the concentration in seawater (40 mBq L^{-1}) at pH values above 7 (Fig. 6A). The
 241 precipitation and/or adsorption of U by the particulate matter was low at pH values lower than 4 and higher than around
 242 6 ($K_d \approx 10^2 - 10^4 \text{ L kg}^{-1}$), while for pH values from 4 to 6, the K_d values were one to two orders of magnitude higher
 243 (Fig. 6B). The abnormal maximum values of K_d ($> 10^5 \text{ L kg}^{-1}$) observed in the Tinto estuary in January and February
 244 are probably due to the increase of U in the particulate matter due to the input of this radionuclide from the PG stacks.
 245 This behaviour has been observed in previous studies (Hsi and Langmuir, 1985; Serkiz and Johnson, 1994) and is
 246 probably due to the coprecipitation of U with Fe-Mn hydroxides (McKee et al., 1987) in the pH range from 4 to 6. On
 247 the other hand, the abnormal increase of dissolved U for pH values > 7 is explained by the existence of redissolution
 248 processes and the formation of carbonated complexes (Hierro et al., 2013). Therefore, in the Odiel and Tinto estuaries,
 249 U shows a non-conservative behaviour.



250

Figure 6. Dissolved ^{238}U activity concentration (A) and ^{238}U distribution coefficients (B) vs pH.

The $^{234}\text{U}/^{238}\text{U}$ activity ratio (AR_U) in the dissolved and particulate phases was also studied (Fig. 7 and Table S8 of the supplementary material). The AR_U in surface waters is generally higher than secular equilibrium ($\text{AR} = 1$) due to nuclide recoil during alpha-decay of ^{238}U and preferential dissolution of ^{234}U (Henderson et al., 2006). The dissolved AR_U presented values above 1 for most of the samples, with higher disequilibrium in the rivers than the estuaries. Mean values of 1.61 and 1.93 were obtained for the Odiel and Tinto rivers respectively (Fig. 7A), with some values higher than 2 in the Tinto River (Fig. 7B) due to more acidic conditions (Barbero et al., 2014; Manjón et al., 2019a). In the Odiel and Tinto estuaries, the mean values in the dissolved phase were 1.21 and 1.11 respectively (Fig. 7A), very near to the value for seawater ($\text{AR}_\text{U} = 1.14$) (Boryło and Skwarzec, 2014). AR_U has a similar and constant value in both estuaries during the year, except for January and February (Fig 7B). During these two months, the percentage of fluvial water at the estuarine points is higher than that in seawater, as was previously described, and therefore an increase of the AR_U is expected, as was observed in the Odiel estuary. On the contrary, the Tinto estuary showed values around secular equilibrium, probably due to the great release of polluted leachates from the PG stacks favoured by the rains, which show AR_U around 1 (Gázquez et al., 2014; Pérez-Moreno et al., 2018).

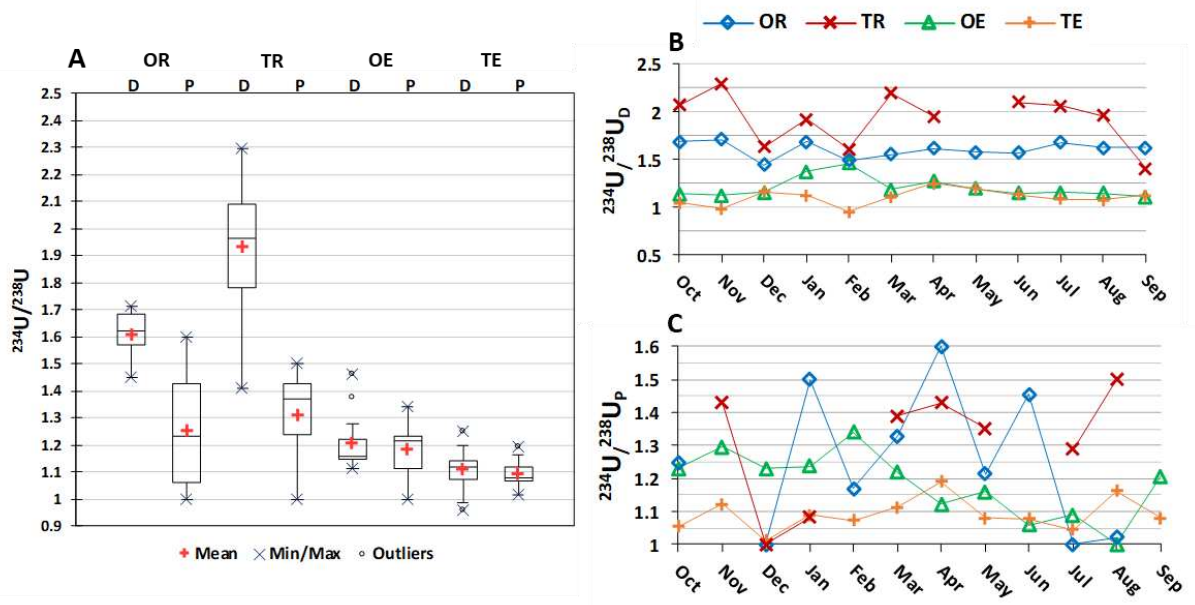


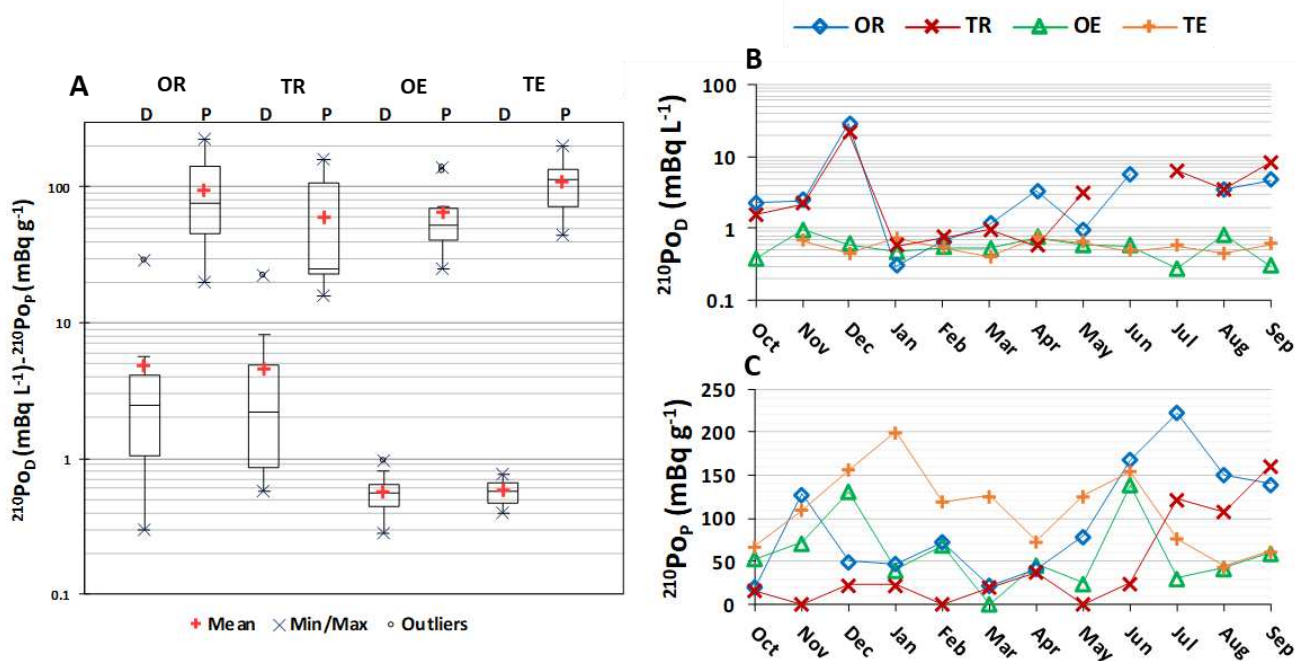
Figure 7. Box whisker plots of the $^{234}\text{U}/^{238}\text{U}$ activity ratio in the dissolved and particulate phases (A), and temporal evolution for the dissolved (B) and particulate phases (C). Central line: median; box limits: first and third quartiles; whiskers: minimum and maximum non-outliers.

Regarding the particulate matter, lower AR_U values than in the dissolved phase were observed at the fluvial points. The mean values for the Odiel and Tinto rivers were 1.25 and 1.31 respectively (Fig. 7A), ranging from values around the

271 secular equilibrium up to higher than 1.5 (Fig. 7C). At the estuarine points, the mean values in the particulate phase
 272 were 1.18 and 1.09 for the Odiel and Tinto estuaries, respectively (Fig. 7A). The lower observed values of this ratio in
 273 the Tinto estuary, mainly during the first half of the studied year (Fig. 7C), are probably once again related to the
 274 influence of the PG stacks.

275 3.3.2 ^{210}Po

276 The activity concentrations of ^{210}Po in the dissolved and particulate phases are shown in Figure 8 and in Table S9 of the
 277 supplementary material. Both rivers and estuaries showed similar dissolved concentrations, with means of around 5 and
 278 0.6 mBq L^{-1} at the fluvial and estuarine points, respectively (Fig. 8A). It highlights the observed dissolved concentration
 279 peaks in December in both rivers, with concentrations higher than 20 and 30 mBq L^{-1} in the Tinto and Odiel rivers,
 280 respectively (Fig. 8B), one order of magnitude higher than background data observed in surface waters (1–5 mBq L^{-1} ;
 281 IAEA, 2017). These peaks are probably related to the dissolution of efflorescences precipitated during the dry months
 282 (Romero et al., 2006; Sánchez España, 2008; Gázquez et al., 2014) by the first rainfalls of the hydrological year (Fig.
 283 S1A, B). In both rivers, the concentrations of dissolved ^{210}Po decrease below 1 mBq L^{-1} during the rainy and increase
 284 again to concentrations from 3 to 8 mBq L^{-1} during the summer. In the estuaries, the concentrations of dissolved ^{210}Po
 285 are approximately constant during the year around the mean value (Fig. 8B) and are similar to the estimated
 286 concentration of this radionuclide in seawater (0.4 to 0.6 mBq L^{-1}) (Skwarzec and Bojanowski, 1988; Uddin et al., 2015)
 287 but slightly lower than the concentration on the coast of Huelva ($\approx 1 \text{ mBq L}^{-1}$) (Bolívar et al., 2000).



288

289 Figure 8. Box whisker plots of the ^{210}Po activity concentration in the dissolved and particulate phases (A), and
290 temporal evolution for the dissolved (B) and particulate phases (C). Central line: median; box limits: first and third
291 quartiles; whiskers: minimum and maximum non-outliers.

292 In the particulate phase, the concentrations showed mean values of 95 and 59 mBq g^{-1} for the Odiel and Tinto rivers,
293 respectively, and 64 and 110 mBq g^{-1} for the Odiel and Tinto estuaries, respectively (Fig. 8A). These concentrations are
294 two to three times higher than the worldwide median value for natural soils (35 mBq g^{-1}) (UNSCEAR 2000). A great
295 dispersion in the concentrations was observed in both rivers and estuaries during the year (Fig. 8C). While the
296 concentrations are higher in the Odiel River than in the Tinto River, in the estuaries the opposite is observed, with higher
297 concentrations in the Tinto estuary, especially during the rainy season. This fact is probably related to the input from
298 the PG stacks due to the high concentration of this radionuclide in the edge outflows from the piles (mean $\approx 2 \cdot 10^4$ mBq
299 L^{-1}) (Pérez-Moreno et al., 2018). The ^{210}Po shows greater association with the particulate matter than ^{238}U (Table S10
300 of the supplementary material). The mean values were 25 and 23% in the Odiel and Tinto rivers, respectively, with the
301 highest values during the winter months, as in the case of ^{238}U . A percentage above 60% was obtained in both rivers in
302 January, while during the month of February a percentage above 90% was obtained for the Odiel River. The mean values
303 increased up to 59 and 77% in the Odiel and Tinto estuaries, respectively. These higher percentages of ^{210}Po are
304 indicative of the lower solubility of this radionuclide under estuarine conditions.

305 ^{210}Po tends to decrease its activity concentration in the dissolved phase with an increase in the pH in the studied rivers
306 ($\text{pH} < 4$), similarly to ^{238}U . The dissolved ^{210}Po shows values < 1 mBq L^{-1} in both rivers and estuaries at pH values > 4 ,
307 and unlike U, does not show an increase in the concentrations at pH values above 6 (Figure 9A). In this sense, Figure
308 9B shows values of K_d one order of magnitude lower ($10^4 - 10^5$ L kg^{-1}) at pH below 4 than at higher pH > 4 ($> 10^5$ L kg^{-1}).
309 These facts demonstrate that ^{210}Po tends to (co)precipitate or to be adsorbed by the particulate matter for pH values
310 higher than 4, showing a non-conservative behaviour. The K_d values are one to two orders of magnitude higher than
311 those of the ^{238}U for the same pH values, which confirms its lower solubility.

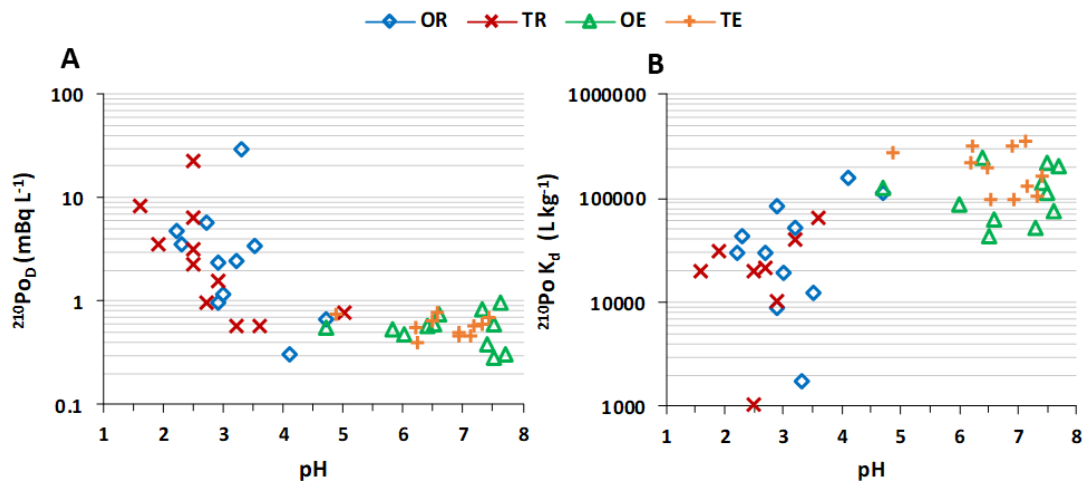
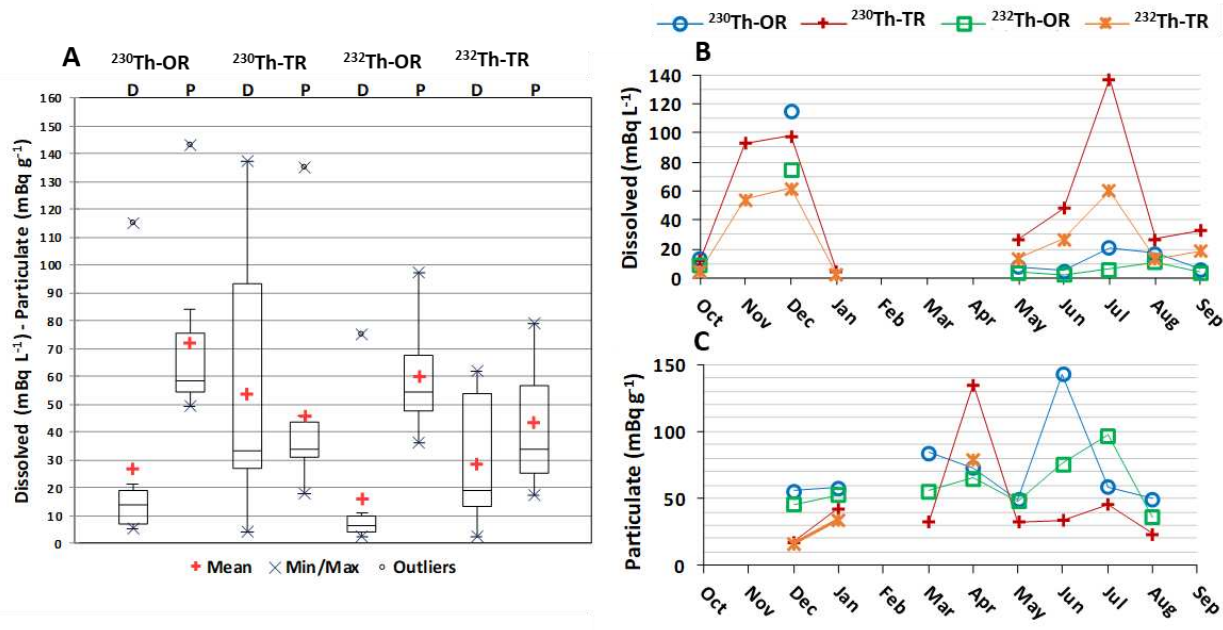


Figure 9. Dissolved ^{210}Po activity concentration (A) and ^{210}Po distribution coefficients (B) vs pH.

3.3.3 Th-isotopes

The results obtained for $^{232,230}\text{Th}$ activity concentration in the rivers are shown in Figure 10. In many cases concentrations below the DL were obtained (Tables S11 and S12 of the supplementary material). Th has a low solubility under neutral conditions, but in waters affected by AMD, due to the high acidity and sulfate concentrations, tends to form soluble sulfate complexes such as $\text{Th}(\text{SO}_4)^{2+}$ and $\text{Th}(\text{SO}_4)_{2(\text{aq})}$ (Kim and Osseo-Asare, 2012). Considering only the detected samples, the dissolved phase showed mean concentrations of ^{230}Th and ^{232}Th of 27 and 16 mBq L^{-1} and 53 and 29 mBq L^{-1} in the Odiel and Tinto rivers, respectively (Fig. 10A). The Tinto River generally showed higher dissolved concentrations than the Odiel River, with a maximum of 50 mBq L^{-1} of ^{232}Th and 100 mBq L^{-1} of ^{230}Th , three to four orders of magnitude higher than in surface continental waters (Zhang et al., 2004; Amrane and Oufni 2017; Manjón et al., 2019b). In the estuaries, the dissolved concentrations of these radionuclides were below the DL ($\approx 0.5\text{-}1 \text{ mBq L}^{-1}$) (Tables S11 and S12), which indicates that Th tends to precipitate due to its high particle reactivity (Wei et al., 2011), showing a non-conservative behaviour in the estuary.

The dissolved concentrations of Th-isotopes also showed a clear seasonal pattern in these rivers, with maxima during the end of autumn and early winter (before the first rains) and during the summer and were below the DL during the rainy season (Fig. 10B). As in the cases of U and Po, this pattern could be explained by three different stages during the year: 1) concentration peaks observed during November and December, probably related to the “washing effect” of salts and efflorescences produced by the first rainfalls after the summer, 2) a “dilution effect” by runoff in the rainy winter, and 3) a progressive “concentration effect” during the spring and summer.



332

333 Figure 10. Box whisker plots of the $^{230,232}\text{Th}$ activity concentration in the dissolved (D) and particulate (P) phases (A),
 334 and temporal evolution of the dissolved (B) and particulate phases (C). Central line: median; box limits: first and third
 335 quartiles; whiskers: minimum and maximum non-outliers.

336 The particulate matter of the rivers showed mean concentrations of ^{230}Th and ^{232}Th of 70 and 60 mBq g⁻¹ and 46 and 43
 337 mBq g⁻¹ in the Odiel and Tinto rivers, respectively. At the estuarine points, similar concentrations were observed, with
 338 means of ^{230}Th and ^{232}Th of 43 and 17 mBq g⁻¹ and 35 and 18 mBq g⁻¹ in the Odiel and Tinto estuaries, respectively (Fig.
 339 10A). Despite the abnormally high concentrations of Th-isotopes in the dissolved phase of the rivers, the activity
 340 concentrations of ^{232}Th in the particulate phase of the estuarine points are in agreement with the worldwide median
 341 concentration in unpolluted soils which is 30 mBq g⁻¹ (range: 11-64 mBq g⁻¹) (UNSCEAR, 2000). This could indicate
 342 that the precipitation of Th occurs at a point previous to the sampling one. In the rivers, the highest concentrations in
 343 the particulate phase were observed during the spring and summer (> 130 mBq g⁻¹ of ^{230}Th), with higher values in the
 344 Odiel River (Fig. 10C). The estuarine points show a low variability during the year, with slightly higher concentrations
 345 during the winter months. For Th-isotopes, the influence of the PG stacks on the Tinto estuary is not observed, probably
 346 due to the low concentrations of these radionuclides in the edge outflows (< 100 mBq L⁻¹) (Pérez-Moreno et al., 2018).

347 4. Conclusions

348 The evolution and behaviour of U-Th-isotopes and ^{210}Po in two rivers affected by AMD and their common polluted
 349 estuary during a year were studied. The conclusions obtained were as follows:

- 350 1. The Odiel and Tinto rivers show concentrations of U-Th isotopes and ^{210}Po from one to three orders of magnitude
 351 higher than background continental waters due to the impact produced by the AMD. ^{238}U showed a mean concentration

352 of around 50 mBq L⁻¹ in these rivers, with maxima above 100 mBq L⁻¹. ²¹⁰Po showed a mean concentration around 5
353 mBq L⁻¹ with maxima above 20 mBq L⁻¹. ²³⁰Th and ²³²Th showed maxima above 100 and 50 mBq L⁻¹, respectively.

354 2. The dissolved AR_U presented high disequilibrium in these AMD polluted rivers, with mean values of 1.6 and 1.9 in
355 the Odiel and Tinto rivers, respectively, and maxima above 2, while in both estuaries a similar mean value to seawater
356 was obtained (AR_U ≈ 1.1).

357 3. The studied radionuclides show a clear seasonal behaviour in these rivers, with three different stages during the year:
358 1) concentration peaks observed during November and December due to the “washing effect” produced by the first
359 rainfalls of the hydrological year, which dissolve the salts and efflorescences precipitated during the dry season, 2) a
360 “dilution effect” by runoff in the rainy winter, and 3) a progressive “concentration effect” during the spring and summer.

361 4. A non-conservative behaviour of the analysed radionuclides in the estuarine mixing zone was demonstrated due to
362 precipitation processes as a result of the increase of pH. The particulate phase of the estuaries is mainly enriched in U-
363 isotopes and ²¹⁰Po, with values around one order of magnitude higher than in unpolluted sediments. Maxima of ²³⁸U and
364 ²¹⁰Po above 10³ and 10² mBq g⁻¹, respectively, were observed.

365 5. The polluted outflows from the PG stacks produce a significant radioactive impact on the Tinto estuary, mainly during
366 the rainiest months, increasing the concentration of U-isotopes and ²¹⁰Po in the particulate matter due to the high
367 concentrations of these radionuclides in the releases and consequent precipitation after the mixing.

368 **5. Funding**

369 This work was partially supported by the Spanish Ministry of Economy and Competitiveness [project number,
370 CTM2015-68628-R] the Spanish Ministry of Science, Innovation and Universities [project number, EQC2018-004306-
371 P], the Regional Government of Andalusia [project number, FEDER2018-UHU-1255876] and the Spanish Ministry of
372 Education [grant number, FPU15/00646]

373 **6. References**

374 Achterberg, E. P., Herzl, V. M., Braungardt, C. B., and Millward, G. E., 2003. Metal behaviour in an estuary polluted
375 by acid mine drainage: the role of particulate matter. *Environ. Poll.*, 121(2), 283–292. doi:10.1016/s0269-
376 7491(02)00216-6

377 Amrane, M., Oufni, L., 2017. Determination for levels of uranium and thorium in water along Oum Er-Rabia River
378 using alpha track detectors. *J. Radiat. Res. Appl. SC.*, 10(3), 246–251. doi:10.1016/j.jrras.2017.05.002

379 Barbero, L., Gázquez, M. J., Bolívar, J. P., Casas-Ruiz, M., Hierro, A., Baskaran, M., Ketterer, M. E., 2014. Mobility
380 of Po and U-isotopes under acid mine drainage conditions: an experimental approach with samples from Río
381 Tinto area (SW Spain). *J. Environ. Radioact*, 138, 384–389. doi:10.1016/j.jenvrad.2013.11.004

382 Blasco, M., Gázquez, M. J., Pérez-Moreno, S. M., Grande, J. A., Valente, T., Santisteban, M., de la Torre, M.L., Bolívar,
383 J. P., 2016. Polonium behaviour in reservoirs potentially affected by acid mine drainage (AMD) in the Iberian
384 Pyrite Belt (SW of Spain). *J. Environ. Radioact*, 152, 60–69. doi:10.1016/j.jenvrad.2015.11.008.

385 Bolívar, J. P., García-Tenorio, R., García-León, M., 1996. On the fractionation of natural radioactivity in the production
386 of phosphoric acid by the wet acid method. *J. Radioanal. Nucl. Chem.*, 214(2), 77–88. doi:10.1007/bf02164808

387 Bolívar, J., 2000. Radioecological study of an estuarine system located in the south of Spain. *Water Res.*, 34(11), 2941–
388 2950. doi:10.1016/s0043-1354(99)00370-x

389 Bolívar, J. P., Martín, J. E., García-Tenorio, R., Pérez-Moreno, J. P., Mas, J. L., 2009. Behaviour and fluxes of natural
390 radionuclides in the production process of a phosphoric acid plant. *Appl. Radiat. Isotopes*, 67(2), 345–356.
391 doi:10.1016/j.apradiso.2008.10.012

392 Boryło, A., and Skwarzec, B., 2014. Activity disequilibrium between ^{234}U and ^{238}U isotopes in natural environment. *J.*
393 *Radioanal. Nucl. Ch.*, 300(2), 719–727. doi:10.1007/s10967-014-3001-9

394 Braungardt, C. B., Achterberg, E. P., Elbaz-Poulichet, F., Morley, N. H., 2003. Metal geochemistry in a mine-polluted
395 estuarine system in Spain. *Appl. Geochem.*, 18(11), 1757–1771. doi:10.1016/s0883-2927(03)00079-9

396 Cánovas, C. R., Olías, M., Nieto, J. M., Sarmiento, A. M., and Cerón, J. C., 2007. Hydrogeochemical characteristics of
397 the Tinto and Odiel Rivers (SW Spain). Factors controlling metal contents. *Sci. Total Environ.*, 373(1), 363–
398 382. doi:10.1016/j.scitotenv.2006.11.022

399 Cánovas, C. R., Olías, M., Nieto, J. M., and Galván, L., 2010. Wash-out processes of evaporitic sulfate salts in the Tinto
400 River: Hydrogeochemical evolution and environmental impact. *Appl. Geochem.*, 25(2), 288–301.
401 doi:10.1016/j.apgeochem.2009.11.014

402 Carro, B., Borrego, J., López-González, N., Grande, J.A., Gómez, T., de la Torre, M.L., Valente, T., 2011. Impact of
403 acid mine drainage on the hydrogeochemical characteristics of the Tinto–Odiel Estuary (SW Spain). *J. Iber.*
404 *Geol*, 37(1):87–96. doi: 10.5209/rev_JIGE.2011.v37.n1.6

405 De Vos, W., Tarvainen, T., 2006. The Geochemical Atlas of Europe Part 2. Interpretation of Geochemical Maps,
406 Additional Tables, Figures, Maps, and Related Publications. 690 pp.

407 Directive, 2013. 2013/59/Euratom of 5 December 2013 Laying Down Basic Safety Standards for Protection against the
408 Dangers Arising from Exposure to Ionising Radiation, and Repealing Directives 89/618/Euratom,
409 90/641/Euratom, 96/29/Euratom, 97/43/Euratom and 2003/122/Euratom.

410 Durand, J. F., 2012. The impact of gold mining on the Witwatersrand on the rivers and karst system of Gauteng and
411 North West Province, South Africa. *J. Afr. Earth Sci.*, 68, 24–43. doi:10.1016/j.jafrearsci.2012.03.013.

412 Fernandes, H. M., Franklin, M. R., Veiga, L. H., 1998. Acid rock drainage and radiological environmental impacts. A
413 study case of the Uranium mining and milling facilities at Poços de Caldas. *Waste Manag.*, 18(3), 169–181.
414 doi:10.1016/s0956-053x(98)00019-1

415 Gázquez, M. J., Mantero, J., Mosqueda, F., Bolívar, J. P., García-Tenorio, R., 2014. Radioactive characterization of
416 leachates and efflorescences in the neighbouring areas of a phosphogypsum disposal site as a preliminary step
417 before its restoration. *J. Environ. Radioact.*, 137, 79–87. doi:10.1016/j.jenvrad.2014.06.025.

418 Gordeev, V. V., Lisitzin, A. P., 2014. Geochemical interaction between the freshwater and marine hydrospheres. *Russ.*
419 *Geol. Geophys.*, 55(5-6), 562–581. doi:10.1016/j.rgg.2014.05.004

420 Henderson, G. M., Hall, B. L., Smith, A., Robinson, L. F., 2006. Control on ($^{234}\text{U}/^{238}\text{U}$) in lake water: A study in the
421 Dry Valleys of Antarctica. *Chem. Geol.*, 226(3-4), 298–308. doi:10.1016/j.chemgeo.2005.09.026

422 Hierro, A., Bolivar, J. P., Vaca, F., Borrego, J., 2012. Behavior of natural radionuclides in surficial sediments from an
423 estuary impacted by acid mine discharge and industrial effluents in Southwest Spain. *J. Environ. Radioact.*, 110,
424 13–23. doi:10.1016/j.jenvrad.2012.01.005

425 Hierro, A., Martín, J. E., Olías, M., Vaca, F., Bolivar, J. P., 2013. Uranium behaviour in an estuary polluted by mining
426 and industrial effluents: The Ría of Huelva (SW of Spain). *Water Res.*, 47(16), 6269–6279.
427 doi:10.1016/j.watres.2013.07.044.

428 Hierro, A., Olías, M., Ketterer, M. E., Vaca, F., Borrego, J., Cánovas, C. R., Bolívar, J. P., 2014. Geochemical behavior
429 of metals and metalloids in an estuary affected by acid mine drainage (AMD). *Environ. Sci. Pollut. R.*, 21(4),
430 2611–2627. doi:10.1007/s11356-013-2189-5

431 Hsi, D., Langmuir, D., 1985. Adsorption of uranyl onto ferric oxyhydroxides: Application of the surface complexation
432 site-binding model. *Geochim. Cosmochim. AC.*, 49(9), 1931–1941. doi:10.1016/0016-7037(85)90088-2

433 IAEA, 2003. Extent of environmental contamination by naturally occurring radioactive material (NORM) and
434 technological options for mitigation. Technical Reports Ser. N° 419.

435 IAEA, 2017. The Environmental behaviour of Polonium. Technical Reports Ser. N° 484.

436 Kennish, M.J., 2017. *Ecology of Estuaries: Volume 1: Physical and Chemical Aspects*. CRC Press. 264 pp.

437 Kim, E., Osseo-Asare, K., 2012. Aqueous stability of thorium and rare earth metals in monazite hydrometallurgy: Eh–
438 pH diagrams for the systems Th–, Ce–, La–, Nd– (PO₄)–(SO₄)–H₂O at 25°C. *Hydrometallurgy*, 113-114, 67–
439 78. doi:10.1016/j.hydromet.2011.12.007

440 Ku, T. L., Knauss, K. G., Mathieu, G. G., 1977. Uranium in open ocean: concentration and isotopic composition. *Deep*
441 *Sea Research*, 24(11), 1005–1017. doi:10.1016/0146-6291(77)90571-9

442 Leblanc, M., Morales, J.A., Borrego, J., Elbaz-Poulichet, E., 2000. 4500-year-old mining pollution in southwestern
443 Spain: long-term implications for modern mining pollution. *Econ. Geol.*, 95, 655-662.
444 doi:10.2113/gsecongeo.95.3.655

445 Loder, T. C., Reichard, R. P., 1981. The Dynamics of Conservative Mixing in Estuaries. *Estuaries*, 4(1), 64.
446 doi:10.2307/1351543

447 Manjón, G., Mantero, J., Vioque, I., Galván, J., Díaz-Francés, I., García-Tenorio, R., 2019a. Some naturally occurring
448 radionuclides (NORM) in a River affected by acid mining drainages. *Chemosphere*.
449 doi:10.1016/j.chemosphere.2019.02.059

450 Manjón, G., Mantero, J., Vioque, I., Díaz-Francés, I., Galván, J. A., Chakiri, S., Choukric, A., and García-Tenorio, R.,
451 2019b. Natural radionuclides (NORM) in a Moroccan river affected by former conventional metal mining
452 activities. *J. Sustain. Min.*, 18(1), 45–51. doi:10.1016/j.jsm.2019.02.003

453 Madzivire, G., Maleka, P. P., Vadapalli, V. R. K., Gitari, W. M., Lindsay, R., Petrik, L. F., 2014. Fate of the naturally
454 occurring radioactive materials during treatment of acid mine drainage with coal fly ash and aluminium
455 hydroxide. *J. Environ. Manage.*, 133, 12–17. doi:10.1016/j.jenvman.2013.11.041.

456 McKee, B. A., DeMaster, D. J., Nittrouer, C. A., 1987. Uranium geochemistry on the Amazon shelf: Evidence for
457 uranium release from bottom sediments. *Geochim. Cosmochim. AC.*, 51(10), 2779–2786. doi:10.1016/0016-
458 7037(87)90157-8

459 Más, J. L., San Miguel, E. G., Bolívar, J. P., Vaca, F., Pérez-Moreno, J. P., 2006. An assay on the effect of preliminary
460 restoration tasks applied to a large TENORM wastes disposal in the south-west of Spain. *Sci. Total Environ.*,
461 364(1-3), 55–66. doi:10.1016/j.scitotenv.2005.11.006

462 Nieto J.M., Sarmiento A.M., Olías M., Cánovas C.R., Riba I., Kalman J., T. Angel Delvalls T. A., 2007. Acid mine
463 drainage pollution in the Tinto and Odiel rivers (Iberian Pyrite Belt, SW Spain) and bioavailability of the
464 transported metals to the Huelva Estuary. *Sci. Total Environ.* 33 (2007)445-455.

465 Nordstrom, D.K., Wilde, F.D., 1998. Reduction-oxidation potential (electrode method). In: *National Field Manual for*
466 *the Collection of Water Quality Data. US Geological Survey Techniques of Water-resources Investigations.*
467 *Book 9, Chap. 6.5.*

468 Olías, M., Nieto, J. M., Sarmiento, A. M., Cerón, J. C., Cánovas, C. R., 2004. Seasonal water quality variations in a
469 River affected by acid mine drainage: the Odiel River (South West Spain). *Sci. Total Environ.*, 333(1-3), 267–
470 281. doi:10.1016/j.scitotenv.2004.05.012

471 Olías, M., Cánovas, C. R., Nieto, J. M., Sarmiento, A. M., 2006. Evaluation of the dissolved contaminant load
472 transported by the Tinto and Odiel rivers (South West Spain). *Appl. Geochem.*, 21(10), 1733–1749.
473 doi:10.1016/j.apgeochem.2006.05.009

474 OSPAR, 2002. Discharges of Radioactive Substances into the Maritime Area by Nonnuclear Industry. *Radioactive*
475 *Substances Series. Publication No. 161. OSPAR Commission, London, 60 pp.*

476 OSPAR, 2007. PARCOM Recommendation 91/4 on Radioactive Discharges: Spanish Implementation Report.
477 *Radioactive Substances Series. Publication No. 342. OSPAR Commission, London, 49 pp.*

478 Papaslioti, E.M., Pérez-López., R, Parviainen, A., Sarmiento, A.M., Nieto, J.M., Marchesi, C., Delgado-Huertas, A.,
479 Garrido. C., 2018. Effects of seawater mixing on the mobility of trace elements in acid phosphogypsum
480 leachates. *Mar. Pollut. Bul.* 127, 695–703. doi:10.1016/j.marpolbul.2018.01.001.

481 Pérez-López, R., Álvarez-Valero, A. M., Nieto, J. M., 2007. Changes in mobility of toxic elements during the production
482 of phosphoric acid in the fertilizer industry of Huelva (SW Spain) and environmental impact of phosphogypsum
483 wastes. *J. Hazard. Mater.*, 148(3), 745–750. doi:10.1016/j.jhazmat.2007.06.068

484 Pérez-López, R., Nieto, J.M, López-Coto, I, Aguado, J.L., Bolívar, J.P., Santiesteban, M., 2010. Dynamics of
485 contaminants in phosphogypsum of the fertilizer industry of Huelva (SW Spain): From phosphate rock ore to
486 the environment. *Appl. Geochem.* 25, 705–715. doi:10.1016/j.apgeochem.2010.02.003.

487 Pérez-López, R., Nieto, J. M., de la Rosa, J. D., Bolívar, J. P., 2015. Environmental tracers for elucidating the weathering
488 process in a phosphogypsum disposal site: Implications for restoration. *J. Hydrol.*, 529, 1313–1323.
489 doi:10.1016/j.jhydrol.2015.08.056

490 Pérez-López R., Macías, F., Cánovas C.R., Sarmiento, A.M., Pérez-Moreno, S.M., 2016. Pollutant flows from a
491 phosphogypsum disposal area to an estuarine environment: An insight from geochemical signatures. *Sci. Total*
492 *Environ.* 553, 42–51. <https://doi.org/10.1016/j.scitotenv.2016.02.070>.

493 Pérez-Moreno, S.M., Gázquez, M.J., Pérez-López, R., Vioque, J., Bolívar, J.P., 2018. Assessment of natural
494 radionuclides mobility in a phosphogypsum disposal area. *Chemosphere* 211, 775-783.
495 doi:10.1016/j.chemosphere.2018.07.193.

496 Porcelli, D., Swarzenski, P.W., 2003. The Behavior of U- and Th-series nuclides in groundwater. *Rev. Mineral.*
497 *Geochem.*, 52(1), 317–361. doi:10.2113/0520317

498 Romero, A., González Díez, I., Galán, E., 2006. The role of Sulphates Efflorescences in the Storage of Trace Elements
499 in stream waters polluted by acid mine drainage. the case of Peña del Hierro (SW Spain). *Canad. Mineral.*,
500 44(6), 1465-1480. doi: 10.2113/gscanmin.44.6.1431

501 Sáez, R., Pascual, E., Toscano, M., Almodóvar, G.R., 1999. The Iberian type of volcano–sedimentary massive sulphide
502 deposits. *Miner. Deposita* 34:549–570.

503 Sánchez España, J., 2008. “Acid mine drainage in the Iberian Pyrite Belt: an overview with special Emphasis on
504 Generation Mechanisms, Aqueous Composition and Associated Mineral Phases,” *Rev. la Soc. Esp. Min.*, vol.
505 10, pp. 34-43.

- 506 Sánchez-Moyano, J. E., García-Asencio, I., and García-Gómez, J. C., 2010. Spatial and temporal variation of the
507 benthic macrofauna in a grossly polluted estuary from southwestern Spain. *Helgol. Mar. Res.*, 64(3), 155–168.
508 doi:10.1007/s10152-009-0175-6
- 509 Serkiz, S.M., Johnson, W.H., 1994. Uranium Geochemistry in Soil and Groundwater at the F and H Seepage Basins
510 (U). EPD-SGS-94-307. Westinghouse Savannah River Company, Savannah River Site, Aiken, South Carolina.
- 511 Skwarzec, B., Bojanowski, R., 1988. ^{210}Po content in sea water and its accumulation in southern Baltic plankton. *Mar.*
512 *Biol.*, 97(2), 301–307. doi:10.1007/bf00391316
- 513 Uddin, S., Aba, A., Fowler, S. W., Behbehani, M., Ismaeel, A., Al-Shammari, H., Alboloushia, A., Mietelskic, J.W.,
514 Al-Ghadbana, A., Al-Ghunaima, A., Khabbaza, A., Alboloushia, A., and Alboloushi, O., 2015. Radioactivity in
515 the Kuwait marine environment — Baseline measurements and review. *Mar. Pollut. Bull.*, 100(2), 651–661.
516 doi:10.1016/j.marpolbul.2015.10.018
- 517 UNSCEAR, 2000. Sources and Effects of Ionizing Radiation. Volume I: Sources: Report to the General Assembly of
518 the United Nations Scientific Committee on the Effects of Atomic Radiation. United Nations, New York.
- 519 Venkateswarlu, K., Nirola, R., Kuppusamy, S., Thavamani, P., Naidu, R., and Megharaj, M., 2016. Abandoned
520 metalliferous mines: ecological impacts and potential approaches for reclamation. *Rev. Environ. Sci. Bio.*,
521 15(2), 327–354. doi:10.1007/s1
- 522 Vicente-Martorell, J. J., Galindo-Riaño, M. D., García-Vargas, M., and Granado-Castro, M. D., 2009. Bioavailability
523 of heavy metals monitoring water, sediments and fish species from a polluted estuary. *J.Hazard. Mater.*, 162(2-
524 3), 823–836. doi:10.1016/j.jhazmat.2008.05.1061157-016-9398-6
- 525 Wei, C.-L., Lin, S.-Y., Sheu, D. D.-D., Chou, W.-C., Yi, M.-C., Santschi, P. H., Wen, L.-S., 2011. Particle-reactive
526 radionuclides (^{234}Th , ^{210}Pb , ^{210}Po) as tracers for the estimation of export production in the South China Sea.
527 *Biogeosciences*, 8(12), 3793–3808. doi:10.5194/bg-8-3793-2011
- 528 Yamamoto, M., Sakaguchi, A., and Kofuji, H., 2010. Uranium in acidic mine drainage at the former Ogoya Mine in
529 Ishikawa Prefecture of Japan. *J. Radioanal. Nucl. Chem.*, 283(3), 699–705. doi:10.1007/s10967-009-0400-4
- 530 Zhang, L., Chen, M., Yang, W., Xing, N., Li, Y., Qiu, Y., Huang, Y., 2004. Size-fractionated thorium isotopes (^{228}Th ,
531 ^{230}Th , ^{232}Th) in surface waters in the Jiulong River estuary, China. *J. Environ. Radioact*, 78(2), 199–216.
532 doi:10.1016/j.jenvrad.2004.05.004